

Robust Zero Modes in Disordered Two-Dimensional Honeycomb Lattice with Kekulé Bond Ordering

Tohru Kawarabayashi^a, Yuya Inoue^a, Ryo Itagaki^a, Yasuhiro Hatsugai^b, Hideo Aoki^{c,d}

^a*Department of Physics, Toho University, Funabashi 274-8510, Japan*

^b*Department of Physics, University of Tsukuba, Tsukuba 305-8571, Japan*

^c*Department of Physics, University of Tokyo, Hongo, Tokyo 113-0033, Japan*

^d*Electronics and Photonics Research Institute, Advanced Industrial Science and Technology (AIST), Tsukuba, Ibaraki 305-8568, Japan*

Abstract

Robustness of zero-modes of two-dimensional Dirac fermions is examined numerically for the honeycomb lattice in the presence of Kekulé bond ordering. The split $n = 0$ Landau levels in a magnetic field as well as the zero-modes generated by topological defects in the Kekulé ordering are shown to exhibit anomalous robustness against disorder when the chiral symmetry is respected.

Keywords: Dirac fermions, chiral symmetry, Kekulé bond ordering

1. Introduction

Graphene [1, 2] has kicked off the physics of Dirac fermions in two dimensions as one of the central issues in the condensed-matter physics [3, 4, 5, 6, 7]. In particular, the characteristic quantum Hall effect is a hallmark of the graphene physics. In the developments of theoretical and experimental understanding of the electronic states for Dirac fermions, there has been a considerable progress in the theoretical studies[8, 9, 10, 11] of the charge fractionalization in two dimensions where fractional and irrational charges emerge in association with the topological defects (vortices) of the Kekulé bond ordering in the honeycomb lattice. Such a system is generally known as a fermion-vortex system having topological zero-energy state in a bulk gap à la Jackiw and Rossi [12]. Experimentally, the Kekulé bond ordering is now realized not only in molecular graphene[13] but also in photonic crystals [14] in a controlled manner enabling us to examine their topological properties.

With such a recent progress in mind, here we explore how disorder will affect the topological zero-energy state associated with the vortex structure in the Kekulé bond ordering in two dimensions, along with the $n = 0$ Landau levels split by the Kekulé ordering. We evaluate the density of states numerically for the lattice model by adopting the Green function method [15] and the kernel polynomial method [16]. To discuss the topological zero-modes induced by topological defects exemplified here by vortices in the Kekulé bond ordering, numerical calculations in large enough systems are necessary for a quantitative analysis. The kernel polynomial method is suitable for obtaining the local density of states accurately in large systems. We have adopted the method to examine not only a single vortex in the bond ordering but also vortices with higher winding numbers and a pair of the vortex and the anti-vortex.

2. Kekulé bond ordering

We consider non-interacting electrons on the two-dimensional honeycomb lattice with the nearest-neighbor hopping t . The energy dispersion is given by $E(\mathbf{k}) = \pm|d(\mathbf{k})|$ with $d(\mathbf{k}) = t[1 + \exp(-ik_1) + \exp(-ik_2)]$, where k_i ($i = 1, 2$) denotes the projection $\mathbf{k} \cdot \mathbf{e}_i$ of the wave vector on the primitive vectors $\mathbf{e}_1 = (\sqrt{3}/2, 3/2)a$ and $\mathbf{e}_2 = (-\sqrt{3}/2, 3/2)a$ (Fig. 1(a)) with a being the nearest-neighbor distance in the honeycomb lattice. The valence and conduction bands touch with each other at K and K' points, $(k_1, k_2) = (-2\pi/3, 2\pi/3)$ and $(2\pi/3, -2\pi/3)$, in the first Brillouin zone, at which $d(\mathbf{k})$ vanishes and a massless Dirac dispersion emerges. The Kekulé bond ordering shown in Fig. 1 (b) folds the K and K' points onto Γ point $(0, 0)$ in the Brillouin zone, at which an energy gap $\pm 3\Delta_K$ at Γ opens. Δ_K is determined by the degree of the Kekulé bond ordering (e.g., the difference in the transfer energy between “thick” and “thin” bonds in a tight-binding model as depicted in Fig.1). The massless Dirac fermions then acquire a mass (in zero magnetic field), despite the fact that the bond ordering does not break the chiral symmetry.

The Kekulé bond ordering for the honeycomb lattice has been discussed as an instability in a strong magnetic field, where the $n = 0$ Landau level splits into $\pm 3\Delta_K$ [17, 18, 19]. Roles of the topological defects in the Kekulé bond ordering have also been discussed for transport properties of graphene in magnetic fields [20].

The tight-binding Hamiltonian for the honeycomb lattice with the nearest-neighbor hopping is given as

$$H = \sum_{\langle i,j \rangle} t_{i,j} e^{-2\pi i \theta_{i,j}} c_i^\dagger c_j + \text{h.c.}$$

in standard notations, where the nearest-neighbor hopping $t_{i,j} = t + t_K + \delta t_{i,j}$ is real. We consider the Kekulé bond ordering given as $t_K = 2\Delta_K$ ($-\Delta_K$) for the thick (thin) bonds in Fig. 1 (b), while $\delta t_{i,j}$ represents a random component which breaks the translational invariance of the system. The magnetic field perpendicular to the system is incorporated as the Peierls phase $\theta_{i,j}$ determined so that the sum of the phases along a closed loop is equal to the magnetic flux enclosed by the loop in units of the flux quantum (h/e). Let us denote the magnetic flux per hexagon as ϕ .

3. Robust $n = 0$ Landau levels

Based on the tight-binding model on the honeycomb lattice, we examine the robustness of the $n = 0$ Landau levels in the presence of the Kekulé bond ordering against an introduction of disorder to the hopping amplitudes which breaks the translational symmetry. In the absence of the Kekulé bond ordering, it has been shown that the $n = 0$ Landau level exhibits an anomalous sharpness when the bond disorder is spatially correlated over several lattice constants [21, 22], which can be understood as a manifestation of the single Dirac fermion property [23], since the scattering between two Dirac fermions at K and K' points is strongly suppressed in such a situation. In the presence of the Kekulé bond ordering, on the other hand, the crucial question is whether or not the anomalous sharpness of the $n = 0$ Landau level is degraded by the strong mixing between K and K' valleys.

We consider a random component $\delta t_{i,j}$ that obeys a Gaussian probability distribution with a variance σ ,

$$P(\delta t_{i,j}) = \frac{1}{\sqrt{2\pi\sigma}} \exp\left(-\frac{\delta t^2}{2\sigma}\right).$$

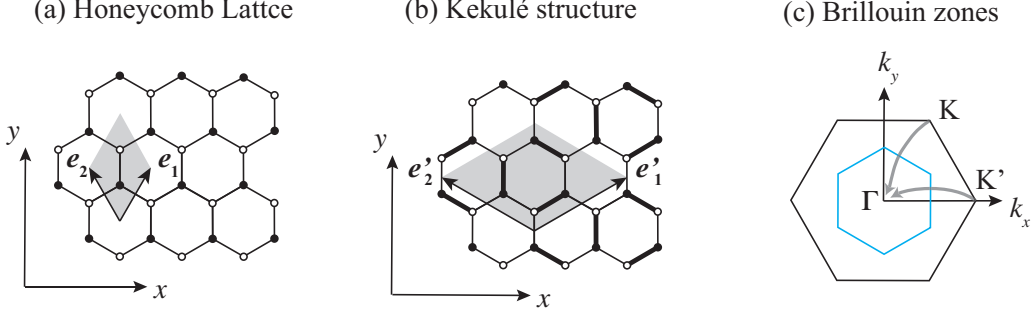


Figure 1: (Color online) (a) The usual honeycomb lattice, for which a unit cell is indicated by the primitive vectors $e_1 = (\sqrt{3}/2, 3/2)a$ and $e_2 = (-\sqrt{3}/2, 3/2)a$ with the distance a between the nearest-neighbor sites. The filled (open) circles represent the A (B) sub-lattice. (b) The honeycomb lattice with the Kekulé bond ordering. The thick (thin) bond represents the hopping amplitude $t+2\Delta_K$ ($t-\Delta_K$). The unit cell is now given by the primitive vectors $e'_1 = (3\sqrt{3}/2, 3/2)a$ and $e'_2 = (-3\sqrt{3}/2, 3/2)a$. (c) The first Brillouin zone for the honeycomb lattice (the outer hexagon) is folded (arrows) onto the inner hexagon (blue) in the presence of the Kekulé bond ordering, where the Brillouin zone becomes 1/3 of the original one and the K and K' points folded onto $\Gamma = (0, 0)$.

The random components are assumed to be spatially correlated as

$$\langle \delta t_{i,j} \delta t_{k,l} \rangle = \langle \delta t^2 \rangle \exp(-(r_{i,j} - r_{k,l})^2 / 4\eta),$$

where η denotes the spatial correlation length and $r_{i,j}$ denotes the spatial position of the bond $t_{i,j}$. We should note that the present disordered system still respects the chiral symmetry.

We evaluate with the Green function method [15] the averaged density of states $\rho(E) = -\langle \text{Im} G_{ii}(E + i\varepsilon) \rangle / \pi$ with $G_{ii}(E) = \langle i | (E - H)^{-1} | i \rangle$, where the angular bracket $\langle \rangle$ denotes the average over the sites i . If we look at the result in Fig. 2, the split $n = 0$ Landau levels at $E = \pm 3\Delta_K$ exhibit an anomalous sharpness as soon as the spatial correlation length η exceeds the nearest-neighbor distance a of the honeycomb lattice. Thus we can conclude that the anomalous robustness of the $n = 0$ Landau levels against the correlated bond disorder survives even in the presence of the valley mixing induced by the Kekulé bond ordering.

To understand the revealed robustness of the $n = 0$ Landau levels, let us consider the effective low-energy Hamiltonian with the in-plane Kekulé distortion, which is given by [17] in a basis (K_A, K_B, K'_A, K'_B) as

$$H_{\text{eff}} = \begin{pmatrix} \gamma(k_x \sigma_x + k_y \sigma_y) & -i\Delta \sigma_y & & \\ i\Delta \sigma_y & \gamma(k_x \sigma_x - k_y \sigma_y) & & \\ & & \gamma(k_x - ik_y) & -\Delta \\ & & \Delta & \gamma(k_x + ik_y) \end{pmatrix} = \begin{pmatrix} 0 & \gamma(k_x - ik_y) & 0 & -\Delta \\ \gamma(k_x + ik_y) & 0 & \Delta & 0 \\ 0 & \Delta & 0 & \gamma(k_x + ik_y) \\ -\Delta & 0 & \gamma(k_x - ik_y) & 0 \end{pmatrix},$$

where σ 's are Pauli matrices, $\Delta \equiv 3\Delta_K$ represents the Kekulé-induced mixing between the K and K' points, and $\gamma = 3at/2$ is a band parameter. In a magnetic field \mathbf{B} , the effective Hamiltonian becomes

$$H_{\text{eff}} = \begin{pmatrix} 0 & \gamma\pi & 0 & -\Delta \\ \gamma\pi^\dagger & 0 & \Delta & 0 \\ 0 & \Delta & 0 & \gamma\pi^\dagger \\ -\Delta & 0 & \gamma\pi & 0 \end{pmatrix}.$$

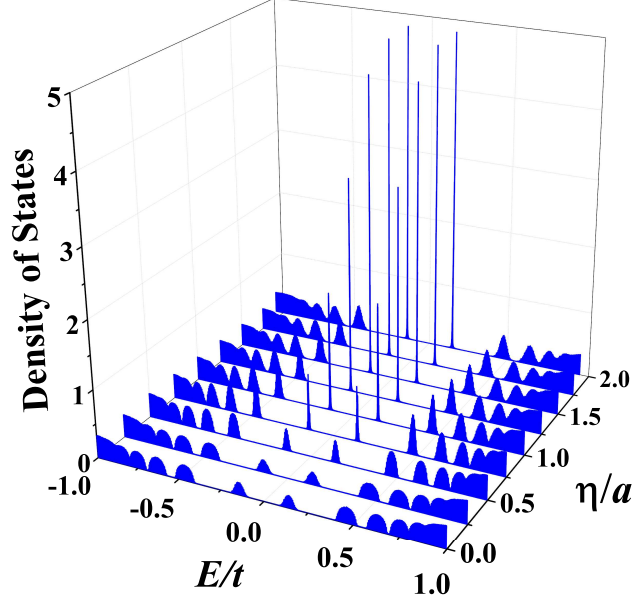


Figure 2: (Color online) Density of states $\rho(E) = -\langle \text{Im}G_{ii}(E + i\epsilon) \rangle / \pi$ for the honeycomb lattice with the Kekulé bond ordering $\Delta_K/t = 0.05$ in a uniform magnetic field $\phi/(h/e) = 1/50$ is plotted for various values of the spatial correlation length η for the random component of the hopping amplitudes. We assume the strength of disorder to be $\sigma/t = 0.115$, and the imaginary part of the energy $\epsilon/t = 6.25 \times 10^{-4}$.

Here $\pi = (p_x - ip_y)/\hbar$, where \mathbf{p} denotes the dynamical momentum $\mathbf{p} = -i\hbar\boldsymbol{\partial} + e\mathbf{A}$, and \mathbf{A} stands for the vector potential with $\nabla \times \mathbf{A} = \mathbf{B}$. The Hamiltonian remains chiral-symmetric, since

$$\Gamma H_{\text{eff}} \Gamma = -H_{\text{eff}} \quad \text{with} \quad \Gamma = \begin{pmatrix} \sigma_z & 0 \\ 0 & \sigma_z \end{pmatrix}.$$

For $\Delta = 0$, the $n = 0$ Landau levels for H_{eff} are exact zero-energy states as given by

$$\psi_0^K = \begin{pmatrix} 0 \\ \phi_0 \\ 0 \\ 0 \end{pmatrix} \quad \text{and} \quad \psi_0^{K'} = \begin{pmatrix} 0 \\ 0 \\ \phi_0 \\ 0 \end{pmatrix}$$

with $\pi\phi_0 = 0$. Note that any linear combinations of those zero-energy eigenstates again belong to the $n = 0$ Landau level.

When the Kekulé distortions are switched on ($\Delta \neq 0$), the zero-modes are split into two Landau levels with energies as

$$H\psi_{\pm} = \pm\Delta\psi_{\pm}.$$

where

$$\psi_+ = \begin{pmatrix} 0 \\ \phi_0 \\ \phi_0 \\ 0 \end{pmatrix} \quad \text{and} \quad \psi_- = \begin{pmatrix} 0 \\ \phi_0 \\ -\phi_0 \\ 0 \end{pmatrix}$$

with $\pi\phi_0 = 0$. As long as the bond disorder is spatially correlated over several lattice constants and hence has little effect on the valley mixing, its effect must appear in the gauge degrees of freedom alone. In such a case, the argument due to Aharonov and Casher [23] may be applied in the same way as in the case of $\Delta = 0$, which implies that those Landau levels are not broadened by disorder.

4. Zero-modes around topological defects

Next, we consider a topological defect (vortex) of the Kekulé bond ordering on the honeycomb lattice, where the topological zero-modes around the vortex emerge in the bulk energy gap [8, 9, 11, 12] irrespective of the presence or absence of uniform magnetic fields perpendicular to the system. In Ref.[19], topological interface states localized along domain boundaries between different realizations of the Kekulé bond ordering have been discussed. If we have three or more realizations, we can have vortices as in Fig.3. For vortices, the number of topological modes at $E = 0$ is equal to the winding number of the vortex. To carry out a quantitative analysis on the zero-modes associated with the topological defects, large systems are examined with the kernel polynomial method [16] where we can look into systems having as large as 10^6 lattice sites. In the implementation, we take the Chebyshev polynomials up to 8200-th order with the Jackson kernel for the evaluation of the local density of states [16].

Taking advantage of the large system sizes, we examine the robustness against disorder of the topological zero-modes not only for a single vortex with the winding number $n_w = 1$ but also for the vortices with higher winding numbers $n_w > 1$. We also examine the effect of disorder for the topological zero modes for a pair of a vortex and an anti-vortex. In actual numerical calculations, we place the topological structure in the central region of our system and adopt the open boundary condition at the boundary. As we shall see in the following, the boundary effect is negligible as long as we discuss the topological zero-modes localized in the central region of the system.

4.1. Zero-modes for a single vortex

We first study the robustness of the zero-mode generated by a single vortex with the simplest winding number $n_w = 1$ illustrated in Fig. 3(a). To see the effect of spatial correlation of the bond disorder $\delta t_{i,j}$, we again assume that $\delta t_{i,j}$ is Gaussian-distributed with a variance σ with the spatial correlation length η as in the previous section. The numerical results with the kernel polynomial method are shown in Figs 3(b), 4 and 5. Figure 3 (b) shows that the zero-mode wave function is spatially localized around the vortex, and resides only on the A sub-lattice. The local density of states at the center site of the vortex in a magnetic field is shown in Fig. 4. It is clearly seen that, irrespective of whether the spatial correlation of the bond disorder is long-ranged ($\eta/a = 2$) or short-ranged ($\eta/a = 0$), the zero-mode associated with the vortex exhibits a sharp peak at $E = 0$, suggesting that the energy of the zero-mode is unaffected by the bond disorder. The result also suggests that the spatial correlation of disorder is insignificant for the robustness of the zero-modes induced by the vortex. We therefore confine ourselves to the spatially uncorrelated disorder for the fermion-vortex system in the following. To confirm the accuracy of the present numerical approach with the kernel polynomial method, we also evaluate the local density of states well away from the vortex center, for example in the red shaded region in Fig. 3 (a). In such a region, the effect of the vortex is hardly seen and the Landau levels for the uniform Kekulé bond ordering are recovered [Fig. 5]. In particular, the anomalous sharpness of the $n = 0$ Landau

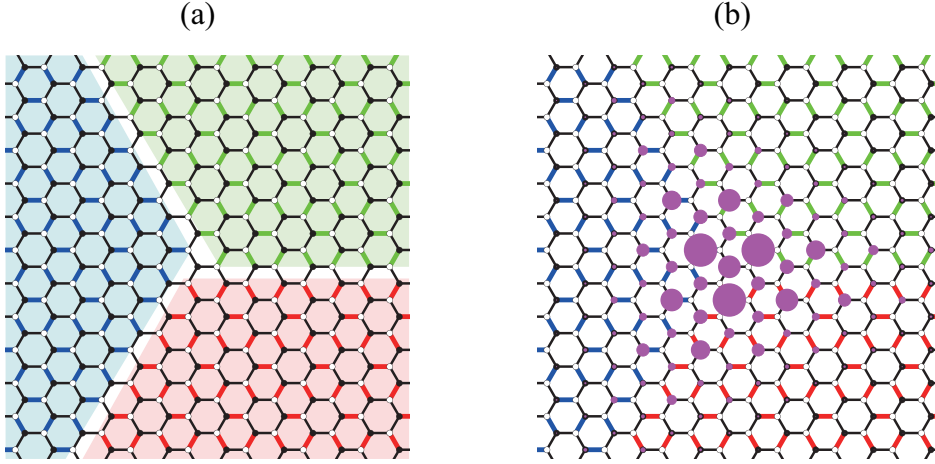


Figure 3: (Color online) (a) A vortex structure of the Kekulé bond ordering with the winding number $n_w = 1$. Hopping amplitudes with $t + 2\Delta_K$ are indicated by thick blue, green and red bonds, while those with $t - \Delta_K$ by thin black bonds. The Kekulé patterns in the red, green, and blue regions are shifted from each other by a single primitive vector of the original honeycomb lattice. The mismatch of the three Kekulé patterns creates a topological defect, a vortex. The vortex is assumed to be located at the center of the system which has 10^6 sites in the present study. (b) The amplitudes of the zero-mode wave function $\psi(r)$ around the vortex, where the radius of each purple circle represents $|\psi(r)|$ and the zero-mode resides only on the A sub-lattice for this vortex. The $|\psi(r)|$ satisfies $\sum_r |\psi(r)|^2 = 1$ indicating that the number of zero modes is 1. The result shown here is for the strength of the Kekulé ordering $\Delta/t = 0.15$.

levels is seen to be retained only for long-ranged disorder ($\eta/a = 2$) in Fig. 5(b). This suggests that the present approach has sufficient accuracy for discussing the robustness of the zero-modes.

4.2. Zero-modes for a vortex-antivortex pair

Let us move on to a pair of a vortex with the winding number $n_w = +1$ and an anti-vortex with $n_w = -1$ as depicted in Fig. 6 (a). When the vortex and anti-vortex are close to each other, the zero-modes are shown in Fig. 6 (b) to split into two. The splitting is expected to be a consequence of the mixing between the vortex zero-mode and the anti-vortex zero-mode. Indeed, the inset of Fig. 6(b) indicates that the splitting energy ΔE decays exponentially with the distance d between the vortices as $\Delta E \propto \exp(-d/\xi_0)$. The decay length is estimated to be $\xi_0 \simeq 10a$ for the case of $\Delta/t = 0.15$, which is in good agreement with the localization length of the zero-mode wave function given as γ/Δ [8] for the effective Hamiltonian H_{eff} .

We then examine the effect of disorder by adding a spatially uncorrelated bond disorder. The local density of states at the center site of the vortex is shown in Fig. 7 for various values of the distance between the vortices, d . We can clearly see that the disorder degrades the sharpness of the split zero-modes when the vortices are close to each other. The sharpness is recovered as d is increased, where the splitting becomes small. The result indicates that the distance between vortex and anti-vortex has to be larger than the localization length of the zero-mode for the robustness of the zero-mode.

4.3. Zero-modes for vortices having higher winding numbers

So far we have considered the simplest winding number $n_w = 1$. How about the vortices having higher winding numbers? So let us look at the result with the winding number for $n_w = 2$

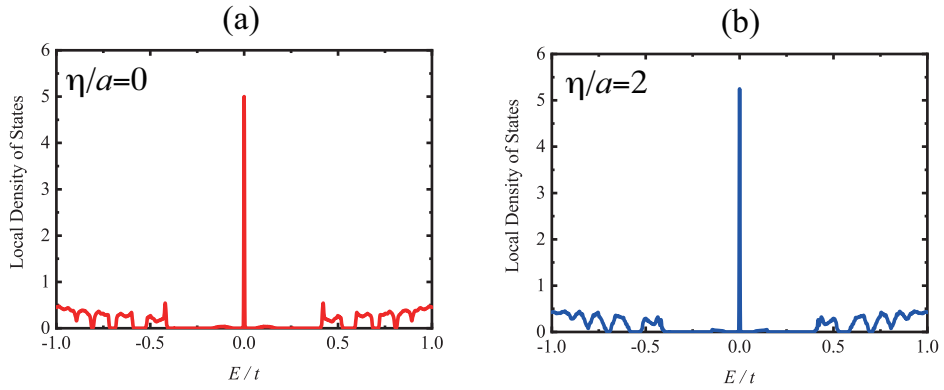


Figure 4: (Color online) The local density of states $\rho(E)$ at the center of the vortex with $\Delta/t = 0.15$ depicted in Fig. 3, evaluated by the kernel polynomial method. The uniform external magnetic field perpendicular to the system is $\phi/(h/e) = 1/50$, and the strength of the bond disorder is $\sigma/t = 0.1$. An average over 100 realizations of disorder is performed. Results for (a) $\eta = 0$ (short-ranged) and (b) $\eta/a = 2$ (long-ranged) are shown.

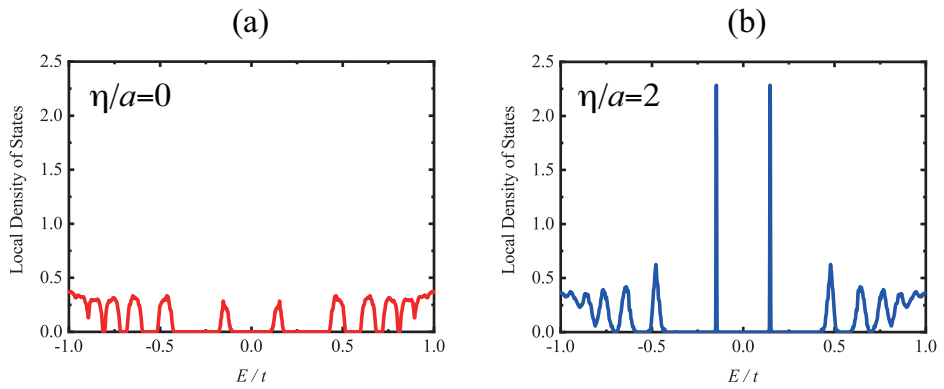


Figure 5: (Color online) The local density of states $\rho(E)$ (~ 200 sites) away from the center of the vortex in Fig. 3, with the parameters the same as in Fig.4.

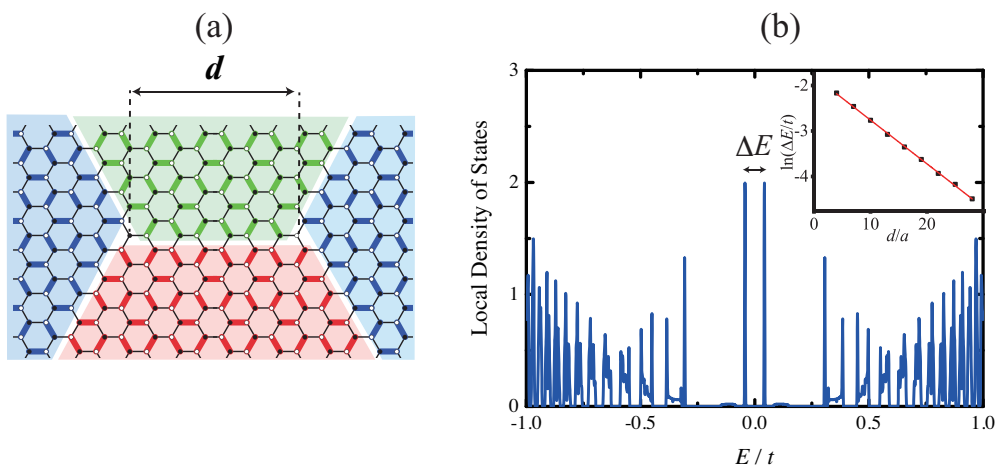


Figure 6: (Color online) (a) A vortex with $n_w = 1$ on the left and an anti-vortex with $n_w = -1$ on the right separated by a distance d in real space. (b) The local density of states $\rho(E)$ at the center site (A sub-lattice) of the left vortex for the case of $d/a = 4$ in the absence of the bond disorder. The system size and the kernel polynomial method are the same as in previous figures. The strength of the Kekulé bond ordering is assumed to be $\Delta/t = 0.15$, and the magnetic flux per hexagon is $\phi/(h/e) = 1/100$. The inset shows the splitting energy ΔE as a function of the distance d between the vortices.

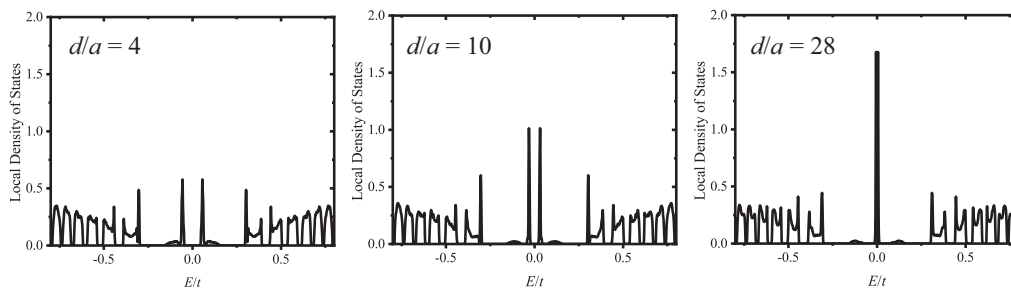


Figure 7: In the presence of a bond disorder the local density of states $\rho(E)$ evaluated at the center site of the vortex illustrated in Fig.6 (a) is shown for the inter-vortex distance $d/a = 4, 10$ and 28 . The disorder is here assumed to be spatially uncorrelated with a uniform distribution over $[-W, W]$ with $W/t = 0.2$. Other parameters are the same as in Fig. 6. An average over 50 realizations of disorder is performed.

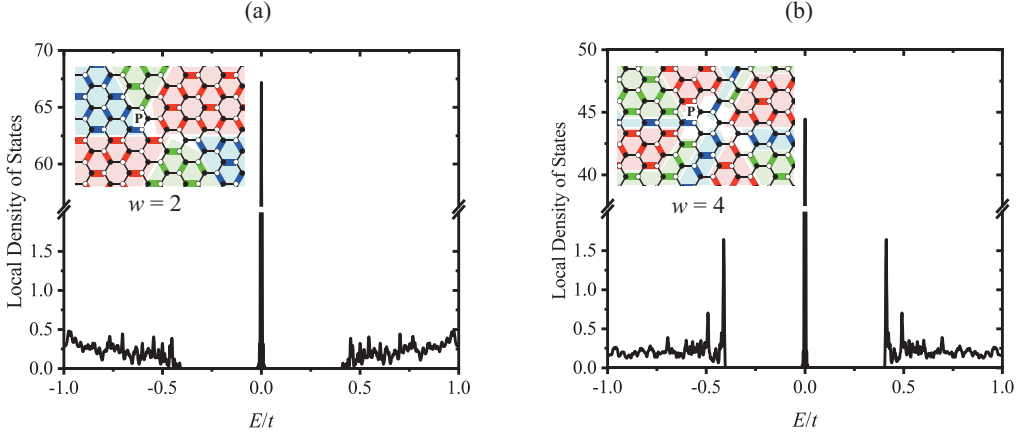


Figure 8: The local density of states $\rho(E)$ at the site P ($\in A$ sub-lattice) located in the central region of the vortex with (a) the winding number $n_w = 2$, and (b) $n_w = 4$ as illustrated respectively in each inset, in zero magnetic field. The strength of the Kekulé bond ordering is $\Delta/t = 0.6$, and a bond disorder, spatially uncorrelated, is considered with a uniform distribution over $[-W, W]$ with $W/t = 0.2$. Here a result for a single realization of disorder is presented.

[Fig. 8(a)] and $n_w = 4$ [Fig. 8(b)], in zero magnetic field to single out the effect of n_w . The local density of states in the central region of the vortex evaluated by the kernel polynomial method is shown in the figure. We can clearly see that the energy of the zero-modes is unaffected by the bond disorder for these higher winding numbers. By evaluating the total amplitude around the vortex, we confirm that the number of zero modes at $E = 0$ is indeed equal to the winding number of the vortex. This indicates that all the zero modes for the vortex with a winding number greater than 1 are degenerated at $E = 0$ even in the presence of the bond disorder. To endorse the topological origin of the zero-modes, we further examined a system with the same winding number but having different bond patterns in the central region of the vortex. We then find that the zero-modes are insensitive to the detailed structure of the central region of the vortex, which suggests that the emergence of the zero-modes at the vortex is indeed dictated by the non-local topological property, such as the winding number, of the vortex structure. All the zero-modes again reside only on the A sub-lattice, and are still the eigenstates of the chiral operator with the eigenvalue 1.

4.4. Staggered potential and irrational charges

What will happen when the chiral symmetry is broken, typically by a staggered potential defined as the Hamiltonian,

$$H_\mu = \mu \left(\sum_{i \in A} c_i^\dagger c_i - \sum_{i \in B} c_i^\dagger c_i \right).$$

When the chiral symmetry is degraded, irrational charges associated with vortices have been discussed [8, 9, 11]. Here we can examine whether the irrational charges remain robust against the bond disorder with direct numerical calculations. Even in the presence of the bond disorder which respects the chiral symmetry, the energy of the zero-mode associated with the vortex must be exactly $E = \mu$, since the zero-mode has amplitudes only on the A sub-lattice, hence an eigenstate of H_μ . This is a direct consequence of the chiral symmetry for $\mu = 0$ that can be confirmed by numerical calculations.

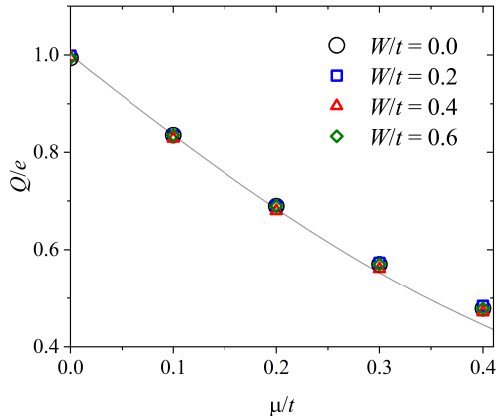


Figure 9: The fractional charge, Q , associated with the vortex with winding number $n_w = 2$ plotted against the staggered potential μ for various values of the strength of disorder W . Spatially uncorrelated bond disorder with a uniform distribution in the range $[-W/2, W/2]$ is adopted. The curve represents the formula $(n_w/2)(1 - \mu/\sqrt{\mu^2 + \Delta^2})$ in Ref. [9].

The charge of a vortex is defined as the increment in the local charge when the vortex is introduced [8]. We evaluate the charge for various values of the disorder strength and the staggered potential μ for the vortices with $w = 1 - 4$. The result indicate that the charge is proportional to the winding number n_w , and insensitive to the strength of the bond disorder. This is exemplified for $n_w = 2$ for various values of the disorder W in Fig. 9. The insensitivity of the irrational charge to disorder may be related to the fact that the bond disorder does not change the energy $E = \mu$ of the zero modes.

5. Summary

We have investigated numerically the honeycomb lattice with the Kekulé bond ordering to examine the robustness of zero-modes against disorder that respects the chiral symmetry. We have clearly shown the following: (i) The split $n = 0$ Landau levels retain the anomalous sharpness as soon as the bond disorder becomes spatially correlated over several lattice constants, which implies that the valley mixing arising from the Kekulé ordering does not impair the sharpness of the $n = 0$ Landau levels. (ii) We have analyzed the topological zero-modes induced by the vortex in the Kekulé bond ordering. With the kernel polynomial method for large systems, the zero-modes induced by the vortex turns out to be robust against the bond disorder irrespective of the presence or the absence of the spatial correlation, confirming the topological stability of the zero-energy states. (iii) We have also analyzed the electronic states around the vortices with higher winding numbers as well as a vortex-antivortex pair. (iv) The fractional and irrational charge is evaluated numerically for vortices with various winding numbers. It is demonstrated that the charge is proportional to the winding number of vortex, in reasonable agreement with the effective theory [9]. The fractional charge is insensitive to the bond disorder that respects the chiral symmetry. It is an interesting future problem how we can relate these with experimentally observable properties.

Acknowledgements

This work is partly supported by JSPS KAKENHI Grants Numbers JP19K03660 (TK), and JP17H06138.

References

- [1] K. S. Novoselov, A. K. Geim, S. V. Morozov, D. Jiang, M. I. Katsnelson, I. V. Grigorieva, S. V. Dubonos, A. A. Firsov, *Nature* **438**, 197 (2005).
- [2] Y. Zhang, Y-W. Tan, H. L. Stormer, P. Kim, *Nature* **438**, 201 (2005).
- [3] A. H. Castro Neto, F. Guinea, N. M. R. Peres, K. S. Novoselov, A. K. Geim, *Rev. Mod. Phys.* **81**, 109 (2009).
- [4] S. Das Sarma, S. Adam, E. H. Hwang, E. Rossi, *Rev. Mod. Phys.* **83**, 407 (2011).
- [5] V. N. Kotov, B. Uchoa, V. M. Pereira, F. Guinea, A. H. Castro Neto, *Rev. Mod. Phys.* **84**, 1067 (2012).
- [6] T. Ando, *J. Phys. Soc. Jpn.* **74**, 777 (2005).
- [7] *Physics of Graphene*, edited by H. Aoki and M. S. Dresselhaus (Springer, Heidelberg, 2014).
- [8] C.-Y. Hou, C. Chamon, and C. Mudry, *Phys. Rev. Lett.* **98**, 186809 (2007); *Phys. Rev. B* **81**, 075427 (2010).
- [9] C. Chamon, C.-Y. Hou, R. Jackiw, C. Mudry, S.-Y. Pi, and A. P. Schnyder, *Phys. Rev. Lett.* **100**, 110405 (2008).
- [10] C. Chamon, C.-Y. Hou, R. Jackiw, C. Mudry, S.-Y. Pi, and G. Semenoff, *Phys. Rev. B* **77**, 235431 (2008).
- [11] S. Ryu, C. Mudry, C.-Y. Hou and C. Chamon, *Phys. Rev. B* **80**, 205319 (2009).
- [12] R. Jackiw and P. Rossi, *Nucl. Phys. B* **190**, 681 (1981).
- [13] K.K. Gomes, et al., *Nature* **483**, 306 (2012).
- [14] Y. Yang, Y. F. Xu, T. Xu, H.-X. Wang, J.-H. Jiang, X. Hu, and Z. H. Hang, *Phys. Rev. Lett.* **120**, 217401 (2018).
- [15] L. Schweitzer, B. Kramer, and A. MacKinnon, *J. Phys. C* **17**, 4111 (1984).
- [16] A. Weisse, et al., *Rev. Mod. Phys.* **78**, 275 (2006).
- [17] N. A. Viet, H. Ajiki and T. Ando, *J. Phys. Soc. Jpn.* **63**, 3036 (1994).
- [18] H. Ajiki and T. Ando, *J. Phys. Soc. Jpn.* **64**, 260 (1994).
- [19] Y. Hatsugai, T. Fukui, and H. Aoki, *Physica E* **40**, 1530 (2008).
- [20] K. Nomura, S. Ryu, and D.-H. Lee, *Phys. Rev. Lett.* **103**, 216801 (2009).
- [21] T. Kawarabayashi, Y. Hatsugai, and H. Aoki, *Phys. Rev. Lett.* **103**, 156804 (2009); *Physica E* **42**, 759 (2010); *Phys. Rev. B* **85**, 165410 (2012).
- [22] T. Kawarabayashi, T. Morimoto, Y. Hatsugai, and H. Aoki, *Phys. Rev. B* **82**, 195426 (2010).
- [23] Y. Aharonov and A. Casher, *Phys. Rev. A* **19**, 2461 (1979).